Inorg. Chem. **2003**, *42*, 436–445

Experimental and Theoretical Study of the Interaction of CO_2 with α-Al_2O_3

Maurizio Casarin,*,† Daniele Falcomer,† Antonella Glisenti,† and Andrea Vittadini‡

Dipartimento di Chimica Inorganica, Metallorganica ed Analitica, Università di Padova, Padova, Italy, and Istituto di Scienze e Tecnologie Molecolari—C.N.R.—Padova, Italy

Received June 7, 2002

Density functional molecular cluster calculations are combined with X-ray photoelectron spectroscopy (XPS), quadrupolar mass spectrometry (QMS), and diffuse reflectance infrared Fourier transform (DRIFT) spectroscopy to investigate the interaction of CO_2 with α-Al_2O_3 and partially reduced α-Al_2O_3. The electronic structure of the stoichiometric and partially reduced substrate, adsorbate geometries, chemisorption enthalpies, and adsorbate vibrational parameters are computed and discussed. Theoretical results agree quite well with experimental data and previous theoretical investigations. As far as the adsorbate–substrate interaction is concerned, the results of our calculations indicate that CO_2 forms bidentate-chelating carbonate species. The bonding scheme of this surface complex implies a significant substrate → adsorbate transfer of charge (from the occupied dangling bond of a surface Lewis base site into one component of the CO_2 $2\pi_u$ LUMO) assisted by a definitely weaker adsorbate → substrate donation (from one component of the CO_2 $1\pi_g$ HOMO into an empty dangling bond of a surface Lewis acid site). Our estimate of the chemisorption enthalpy (–15 kcal/mol) agrees quantitatively with calorimetric data reported for CO_2 adsorbed on high surface area α-alumina (–16.0 kcal/mol). [Mao, C.-F.; Vannice, M. A. *Appl. Catal. A* **1994**, *111*, 151.] According to XPS and QMS outcomes, theoretical results predict that the interaction of CO_2 with partially reduced α-Al_2O_3 gives rise to the reduction of the adsorbate to CO and to the concomitant substrate reoxidation.

1. Introduction

Metal oxides are currently used for several applications of technological interest as a consequence of their electrical behavior (ranging from insulator to superconductor) and catalytic activity.[1] Besides applicative interests, a detailed comprehension of chemisorption processes taking place on metal oxide surfaces is also of great relevance because "the metal cations exposed at the surface of metal oxides have much in common with their counterpart in solution",[2] thus providing the strongest connection between heterogeneous and homogeneous catalysis.

Catalytic reactions on many metal oxide surfaces are broadly classified as acid−base reactions, with the surface playing the role of a solid acid or base.[3] In relation to that, a few years ago Zecchina et al.[4] tackled the problem of giving a general definition of the acid and basic strength of surface sites following both Brønsted and Lewis theories. In particular, they stressed that a reliable scale of surface acidity/basicity can only be obtained if the employed probe molecules weakly interact with surface sites. On this basis, the CO molecule is well suited to probe the Lewis acidity of surface positive centers (hereafter indicated as L_s^a),[5] whereas no standard probe is available for exposed Lewis

* To whom correspondence should be addressed. E-mail: maurizio.casarin@unipd.it. Phone: ++39-049-8275164. Fax: ++39-049-8275161.

† Dipartimento C. I. M. A.—Università di Padova.

‡ I. S. T. M.—CNR di Padova.

(1) (a) Henrich, V. E. *Rep. Prog. Phys.* **1985**, *48*, 1481. (b) Freund, H.-J. *Ber. Bunsen-Ges. Phys. Chem.* **1995**, *99*, 1261. (c) Henrich, V. E.; Cox, P. A. *The Surface Science of Metal Oxides*; Cambridge University Press: Cambridge, England, 1996. (d) Freund, H.-J.; Kuhlenbeck, H.; Staemmler, V. *Rep. Prog. Phys.* **1996**, *59*, 283. (e) Freund, H.-J. *Angew. Chem., Int. Ed. Engl.* **1997**, *36*, 452.

(2) Barteau, M. A. *J. Vac. Sci. Technol., A* **1993**, *11*, 2162.

(3) (a) Stair, P. C. *J. Am. Chem. Soc.* **1982**, *104*, 4044. (b) Spitz, R. N.; Barton, J. E.; Barteau, M A.; Staley, R. H.; Sleight, A. W. *J. Phys. Chem.* **1986**, *90*, 4067.

(4) Zecchina, A.; Lamberti, C.; Bordiga, S. *Catal. Today* **1998**, *41*, 169.

(5) The general consensus about the use of CO derives from the following characteristics of the L_s^a−CO surface complex: (i) the CO molecule results always chemisorbed carbon-end-down oriented; (ii) stretching frequency variations ($\Delta\nu_{CO}$) upon chemisorption can be quite easily related to the oxidation state as well as to the coordination number of exposed L_s^a's;[6] (iii) the formation of the L_s^a−CO surface complex does not perturb significantly the surface relaxation.

10.1021/ic0257773 CCC: $25.00
Published on Web 12/20/2002

base sites (hereafter indicated as L_s^b's). In this regard, it should be stressed that CO_2 has been often proposed for this purpose, but its high acidity favors the formation of stable adducts without allowing a discrimination among L_s^b's of comparable strength.[4] On the other hand, it is worth noting that the interaction/decomposition of CO_2 with/on metal oxide based materials[7] is one of the target technologies for its utilization.

In the past few years, the surface chemistry of α-Al_2O_3 single crystals has been extensively investigated both experimentally and theoretically.[8] Most of these studies dealt with the defect free α-Al_2O_3(0001) basal plane because this surface is stable (it is the α-Al_2O_3 cleavage surface) and very well characterized.[8a−d] At variance to that, polycrystalline α-Al_2O_3 often includes point defects which in principle could modify the sample surface reactivity, and consequently the material performances, in particular, in hostile environments. In this regard, it is noteworthy that very few theoretical studies have addressed the structural and electronic properties of oxygen vacancies (hereafter V_O, often indicated as F centers), one of the most common α-Al_2O_3 defects.[9]

To our knowledge, no theoretical investigation has so far been devoted to the study of the chemisorption of CO_2 on α-Al_2O_3, and the number of experimental contributions dealing with this subject is also quite limited.[11] Moreover, most studies concerning the interaction of CO_2 with alumina have been carried out by employing either hydrated α-Al_2O_3[11] or transition aluminas.[12] In this habit, the strong affinity of α-Al_2O_3 for water[13] is particularly important because the sample hydration degree influences the CO_2−surface interactions. In this regard, Busca and Lorenzelli[11a] and Morterra et al.[11b] have pointed out that the interaction of CO_2 with highly hydroxylated surfaces yields monodentate bicarbonates and carbonates (hereafter, MC), whereas the only species present on anhydrous samples is the bidentate-chelating carbonate (hereafter, BCC; see Figure 1).

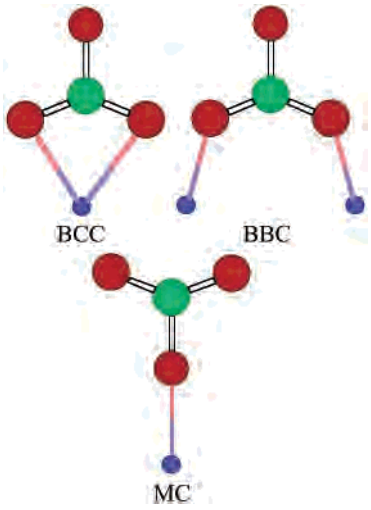

Figure 1. Schematic representation of possible geometries of surface carbonate on α-Al_2O_3. Blue, red and light green, circles correspond to Al, O, and C atoms, respectively. The acronyms MC, BCC, and BBC stand for monodentate carbonate, bidentate-chelating carbonate, and bidentate-bridging carbonate, respectively.

In this contribution, we provide a detailed description of the interaction of CO_2 with stoichiometric and partially reduced α-Al_2O_3 based upon XPS, QMS, and DRIFT data and density functional (DF) calculations. More specifically, the experimental outcomes pertaining to the chemisorption of CO_2 on dehydroxylated surfaces of α-Al_2O_3 have been rationalized by referring to the results of molecular cluster DF calculations.[14] The final goals of the present study are the following: (i) to get a detailed understanding of the chemisorption of CO_2 on anhydrous α-Al_2O_3; (ii) to look into the structural and electronic properties of surface V_O centers; (iii) to investigate the CO_2−V_O interactions.

2. Experimental Section

2.1. Theoretical Model. The α-Al_2O_3(0001) surface is terminated by an Al layer, strongly inward relaxed.[8a−c] Each L_s^a carries three coordinative vacancies and it is bonded to three L_s^b's, each of them missing a single ligand. The overall charge (3/2e) occupying the

(6) Petrie, W. T.; Knözinger, H. *J. Catal.* **1989**, *119*, 311.
(7) Shin, H.-C.; Choi, S.-C.; Jung, K.-D.; Han, S.-H. *Chem. Mater.* **2001**, *13*, 1238.
(8) (a) Ahn, J.; Rabalais, J. W. *Surf. Sci.* **1997**, *388*, 121. (b) Renaud, G. *Surf. Sci. Rep.* **1998**, *32*, 1. (c) Guénard, P.; Renaud, G.; Barbier, A.; Gautier-Soyer, M. *Surf. Rev. Lett.* **1998**, *5*, 321. (d) Puchin, V. E.; Gale, J. D.; Shluger, A. L.; Kotomin, E. A.; Günster, J.; Brause, M.; Kempter, V. *Surf. Sci.* **1997**, *370*, 190. (e) Manassidis, L.; De Vita, A.; Gillan, M. J. *Surf. Sci.* **1993**, *285*, L517. (f) Manassidis, L.; Gillan, M. J. *J. Am. Ceram. Soc.* **1994**, *77*, 335. (g) Wittbrodt, J. M.; Hase, W. L.; Schlegel, H. B. *J. Phys. Chem. B* **1998**, *102*, 6539. (h) Batirev, I. G.; Alavi, A.; Finnis, M. W.; Deutsch, T. *Phys. Rev. Lett.* **1999**, *82*, 1510. (i) Verdozzi, C.; Jennison, D. R.; Schultz, P. A.; Sears, M. P. *Phys. Rev. Lett.* **1999**, *82*, 799. (j) Di Felice, R.; Northrup, J. E. *Phys. Rev. B* **1999**, *60*, 12287. (k) Elam, J. W.; Nelson, C. E.; Cameron, M. A.; Tolbert, M. A.; George, S. M. *J. Phys. Chem. B* **1998**, *102*, 7008. (l) Rodriguez, J. A.; Chaturvedi, S.; Kuhn, M.; Hrbek, J. *J. Phys. Chem. B* **1998**, *102*, 7008. (m) Liu, P.; Kendelewicz, T.; Brown, G. E., Jr.; Nelson, E. J.; Chambers, S. A. *Surf. Sci.* **1998**, *417*, 53. (n) Hass, K. C.; Schneider, W. F.; Curioni, A.; Andreoni, W. *Science* **1998**, *282*, 265. (o) Hass, K. C.; Schneider, W. F.; Curioni, A.; Andreoni, W. *Science* **2000**, *104*, 5227. (p) Casarin, M.; Maccato, C.; Vittadini, A. *Inorg. Chem.* **2000**, *39*, 5232. (q) Baxter, R.; Reinhardt, P.; Lopez, N.; Illas, F. *Surf. Sci.* **2000**, *445*, 448. (r) Wander, A.; Searle, B.; Harrison, N. M. *Surf. Sci.* **2000**, *458*, 25. (s) Nelson, C. E.; Elam, J. W.; Tolbert, M. A.; George, S. M. *Appl. Surf. Sci.* **2001**, *171*, 21. (t) Baudin, M.; Hermansson, K. *Surf. Sci.* **2001**, *474*, 107. (u) Gomes, J. R. B.; Moreira, I. de P. R.; Reinhardt, P.; Wander, A.; Searle, B. G.; Harrison, N. M.; Illas, F. *Chem. Phys. Lett.* **2001**, *341*, 412.
(9) F centers can be either neutral or charged according to the number of electrons trapped in the neighborhood (F^+, F, and F^- correspond to the trap of one, two, or three electrons, respectively). The creation of F centers usually implies the evolution of O_2 which can be formed either by directly releasing oxygen atoms (F) or by creating F centers of opposite charge (F^+ and F^-).[10] Nothing is reported in the literature about the F center reactivity.
(10) (a) Jacobs, P. W.; Kotomin, E. A. *J. Am. Ceram. Soc.* **1994**, *77*, 2505. (b) Xu, Y.-N.; Gu, Z.-Q.; Zhong, X.-F.; Ching, W. Y. *Phys. Rev. B* **1997**, *56*, 7277. (c) Stashans, A.; Kotomin, E. A.; Calais, J.-L. *Phys. Rev. B* **1994**, *49*, 14854. (d) Evans, B. D.; Pogatshnik, G. J.; Chen, Y. *Nucl. Instrum. Methods Phys. Res., Sect. B* **1994**, *91*, 258.
(11) (a) Busca, G.; Lorenzelli, V. *Mater. Chem.* **1982**, *7*, 89. (b) Morterra, C.; Coluccia, S.; Ghiotti, G.; Zecchina, A. *Z. Phys. Chem.* **1977**, *104*, 275. (c) Dewaele, O.; Froment, G. F. *Appl. Catal., A* **1999**, *185*, 203.
(12) (a) Peri, J. B. *J. Phys. Chem.* **1966**, *70*, 3168. (b) Gregg, S. J.; Ramsay, J. D. F. *J. Phys. Chem.* **1969**, *75*, 1243. (c) Parkyns, N. D. *J. Phys. Chem.* **1971**, *75*, 526. (d) Rethwisch, D. G.; Dumesic, J. A. *Langmuir* **1986**, *2*, 73. (e) Auroux, A.; Gervasini, A. *J. Phys. Chem.* **1990**, *94*, 6371. (f) Mao, C.-F.; Vannice, M. A. *Appl. Catal., A* **1994**, *111*, 151. (g) Cascarini de Torre, L. E.; Flores, E. S.; Llanos, J. L.; Bottani, E. J. *Langmuir* **1995**, *11*, 4742.
(13) Ahn and Rabalais[8a] revealed OH surface groups on α-Al_2O_3(0001) surviving at 1100 °C.
(14) As ordinarily done when dealing with α-Al_2O_3,[8k,p,s] the substrate has been modeled by referring to its (0001) surface.

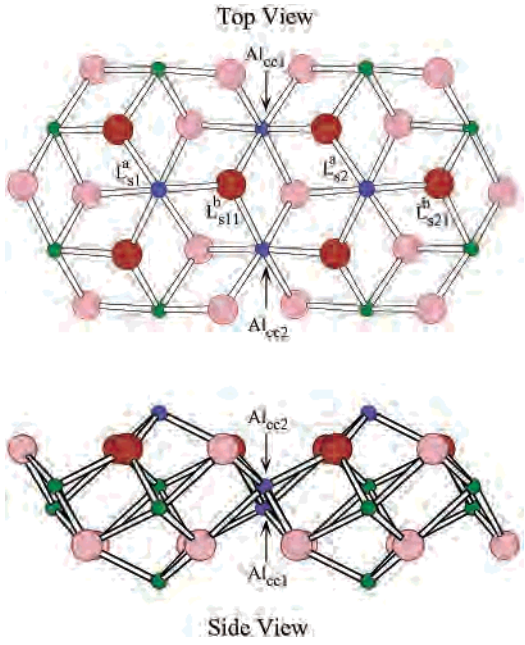

Figure 2. Schematic representation of the unrelaxed cluster $Al_{14}O_{22}$ (**I**). Al (O) atoms in blue (red) are chemically complete while those in green (pink) have pseudo-hydrogen saturators (not displayed for the sake of clarity) as nearest neighbors.

three L_s^a dangling bonds (DBs) can be thought to be transferred to the partially occupied DB of three L_s^b's of the second layer, which then result in being filled by two electrons. As a whole, the number of empty and filled DBs on the α-Al_2O_3(0001) is the same, and the surface is nonpolar.

A few years ago, we investigated the electronic/structural properties of the α-Al_2O_3(0001) surface, as well as its interaction with carbon monoxide (CO), by using the stoichiometric Al_8O_{12} cluster.[8p] In that cluster, all the atoms below the first two layers needed to be saturated (vide infra) so that Al_8O_{12} is unfit to investigate the formation of surface BCC species. A suitable alternative is the larger cluster $Al_{14}O_{22}$ (hereafter **I**, see Figure 2) which consists, as Al_8O_{12}, of six layers (four of aluminum and two of oxygen), but it includes, in the third and fourth layers, chemically complete Al atoms (Al_{CC1} and Al_{CC2} in Figure 2).

Spurious surface states of **I** have been eliminated by saturating all DBs (with the obvious exception of those localized on L_s^a and L_s^b) with pseudo-hydrogen atoms carrying a fractional nuclear charge. The use of pseudo-hydrogen atoms as DB saturators has been successfully applied to model polar and nonpolar surfaces of many different materials such as Cu_2O,[15a−c] Ag_2O,[15a] ZnO,[15d] TiO_2,[15e] Al_2O_3,[9p,15f] Ti_2O_3,[15f] and CuCl.[15g] Moreover, it is worth noting that, among the 11 O atoms of the second layer of **I** (see Figure 2), those colored in pink carry two, rather than one, coordinative vacancies; only one of them needs to be saturated.

To describe the saturation procedure, one has to keep in mind that in the corundum bulk structure Al and O atoms are six- and four-fold coordinated, respectively. This means that each Al formally shares its three valence electrons with six oxygen atoms, thus contributing with 1/2e to each Al−O bond, while O formally participates to the same bond with 3/2e. On this basis, **I** is correctly saturated by providing 3/2e (1/2e) to each Al (O) DB. Such a result can be obtained by employing pseudo-hydrogen saturators having fractional nuclear charges (H′ with $Z = 3/2$, and H″ with $Z = 1/2$). The adopted Al−H′ (1.602 Å) and O−H″ (1.055 Å) bond lengths (BLs) have been obtained by optimizing the geometry of octahedral AlH'_6 and tetrahedral OH''_4 pseudo-molecules. The next step consists of determining the correct number of electrons to fill the cluster energy levels. As already pointed out, the charge of the L_s^a DBs is transferred to the L_s^b DBs. However, in our cluster, there are only two L_s^a with three coordinative vacancies and 11 L_s^b's, each of them carrying a single DB which needs 1/2e to be filled. Thus, the filling of the peripheral L_s^b DBs (those in pink in Figure 2) could be obtained by adding to the saturated cluster a 5/2e charge. Here, we preferred to adopt a different approach. Actually, replacing the 5 H″ saturators of the peripheral L_s^b with hydrogen atoms implies the addition of exactly 5/2e to the cluster levels without affecting the net charge of the system. We already showed in refs 8p and 15e−f that this procedure is preferable because no arbitrary shifts are needed to compare one-electron energy levels.

2.2. Computational Details. All the calculations have been run within the DF theory by using the ADF 1999 packages.[16] Moreover, geometry optimization, adsorption enthalpies, and frequency calculations were obtained by using generalized gradient (GGA) corrections self-consistently included through the Becke−Perdew (BP) formula.[17]

A triple-ζ Slater-type basis set was used for Al, and O and C atoms of CO_2, while for the substrate O atoms and for saturators (pseudo-hydrogen and hydrogen atoms) we used a double-ζ basis. The inner shells of Al (1s2s2p), O (1s), and C (1s) atoms were treated by the frozen-core approximation.

The adsorption enthalpy (ΔH_{ads}) was analyzed in terms of the adsorbate and substrate fragment orbitals by applying Ziegler's extended transition state method[18] (ETS). According to the ETS scheme, the ΔH_{ads} can be written as

$$\Delta H_{ads} = \Delta E_{elstat} + \Delta E_{Pauli} + \Delta E_{int} + \Delta E_{prep} \qquad (2.1)$$

Here, ΔE_{elstat} is the pure electrostatic interaction, ΔE_{Pauli} is the destabilizing two-orbital−four-electron interaction between the occupied orbitals of the two interacting fragments, ΔE_{int} derives from the stabilizing interaction between occupied and empty orbitals of the fragments, and the last term, ΔE_{prep}, is the energy required to relax the structure of the free fragments to the geometry they assume in the final system. Adsorption enthalpies were further corrected by taking into account the basis set superposition error (BSSE), which was estimated through the use of reference energies computed with ghost adsorbate and surface fragments.[19] Finally, force constants and harmonic frequencies were calculated by numerical differentiation of energy gradients computed both at the equilibrium geometry and at slightly deviating geometries.

Information about the localization and the bonding/antibonding character of selected molecular orbitals (MOs) has been obtained

(15) (a) Casarin, M.; Maccato, C.; Vittadini, A. *Chem. Phys. Lett.* **1997**, *280*, 53. (b) Casarin, M.; Maccato, C.; Vittadini, A. *Chem. Phys. Lett.* **1999**, *300*, 403. (c) Casarin, M.; Maccato, C.; Vittadini, A. *Appl. Surf. Sci.* **1999**, *142*, 164. (d) Casarin, M.; Maccato, C.; Vittadini, A. *Inorg. Chem.* **1998**, *37*, 5482. (e) Casarin, M.; Maccato, C.; Vittadini, A. *J. Phys. Chem. B* **1998**, *102*, 10745. (f) Casarin, M.; Maccato, C.; Vittadini, A. *J. Phys. Chem. B* **2002**, *106*, 795. (g) Casarin, M.; Favero, G.; Tondello, E.; Vittadini, A. *Surf. Sci.* **1994**, *317*, 422.

(16) (a) *Amsterdam Density Fuctional Package*, version 1999; Vrjie Universiteit: Amsterdam, The Netherlands, 1999. (b) Baerends, E. J.; Ellis, D. E.; Ros, P. *Chem. Phys.* **1973**, *1*, 41. (c) te Velde, G.; Baerends, E. J. *J. Comput. Chem.* **1992**, *99*, 84. (d) Fonseca Guerra, C.; Visser, O.; Snijders, J. G.; Baerends, E. J. In *Methods and Techniques in Computational Chemistry*; Clementi, E., Corongiu, G., Eds.; STEF: Cagliari, Italy, 1995; Chapter 8, p 305.

(17) (a) Becke, A. D. *Phys. Rev. A* **1988**, *38*, 3098. (b) Perdew, J. P. *Phys. Rev. B* **1986**, *33*, 8822.

(18) Ziegler, T.; Rauk, A. *Theor. Chim. Acta* **1977**, *46*, 1.

(19) Rosa, A.; Ehlers, A. W.; Baerends, E. J.; Snijders, J. G.; te Velde, G. *J. Phys. Chem.* **1996**, *100*, 5690.

by evaluating density of states (DOS), partial DOS (PDOS), and crystal orbital overlap population (COOP).[20] These curves have been computed by applying a Lorentzian broadening factor of 0.25 eV to the one-electron energy levels and by weighting them by their basis orbital percentage.

2.3. Sample Preparation. α-Al_2O_3 was prepared by heating treatment (1523 K for 30 h) of an Al_2O_3 powder (Baker Analyzed, 98.5%).[11b] Before chemisorption in high vacuum (HV) conditions, the sample was processed as a pellet (the powder was pressed at 2 $\times$ 10^8 Pa for 10 min), evacuated for 20 min at room temperature (RT), and then activated by heating at 773 K in HV (pressure $<$ 1 $\times$ 10^{-4} Pa) for 48 h.

2.4. Reaction Conditions. The exposure of the pellet to CO_2 in HV has been carried out at RT (the sample temperature was controlled through a thermocouple directly in contact with the sample-holder) at a total pressure of $\sim$4 $\times$ 10^{-4} Pa. The employed HV reactor, directly connected to the XPS analysis chamber, allowed us to work in flux conditions; moreover, volatile products were characterized by means of a quadrupole gas analyzer (European Spectrometry Systems, ESS). QM spectra were assigned by referring to the fragmentation patterns;[21] furthermore, they were all analyzed by using the method proposed by Ko et al.[22] Background contributions were eliminated by subtracting the spectrum recorded just before the chemisorption to the one obtained after the CO_2 dosing. Water contamination was present, but the comparison between QM spectra recorded before and after the CO_2 exposure indicated a constant amount of contaminant.

The dosing in the FTIR equipment was done at both RT and 523 K by means of the COLLECTOR apparatus for DRIFT spectroscopy from Spectra-Tech, Inc., fitted with the HTHP (high-temperature high pressure) chamber and connecting the CO_2 outlet directly to the reaction chamber.

2.5. DRIFT Measurements. IR spectra were obtained by using a Bruker IFS 66 spectrometer in the diffuse reflectance mode and displayed in Kubelka−Munk units.[23] The resolution of the spectra was 4 cm^{-1}. The temperature of the powder was checked through a thermocouple inserted into the sample holder directly in contact with the powder.

2.6. XPS Measurements. XP spectra were recorded on a Perkin-Elmer PHI 5600-ci spectrometer with a standard Al Kα source (1486.6 eV) working at 350 W. The working pressure was less than 1 $\times$ 10^{-8} Pa. The spectrometer was calibrated by assuming the binding energy (BE) of the Au $4f_{7/2}$ line to be 84.0 eV with respect to the Fermi level. Extended spectra (surveys) were collected in the range 0−1350 eV (187.85 eV pass energy, 0.4 eV per step, 0.05 s per step). Detailed spectra were recorded for the following regions: C(1s), O(1s), Al(2p) (11.75 eV pass energy, 0.1 eV per step, 0.1 s per step). The standard deviation in the BE values of the XPS line was 0.10 eV. The atomic percentage, after a Shirley type background subtraction,[24] was evaluated using the PHI sensitivity factors.[25] To take into account possible charging problems, the C 1s peak was considered at 285.0 eV, and BE differences were evaluated.

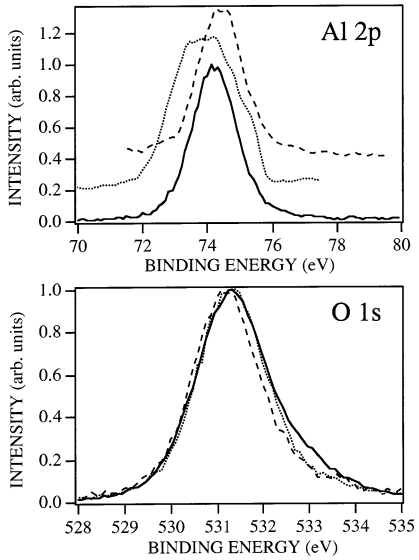

Figure 3. XP spectra of the α-Al_2O_3 powder sample obtained after the treatment at 1423 K (—); after the activation (773 K) under HV conditions (····); after the exposure to CO_2 at RT under HV conditions (- - -).

2.7. Thermal Analysis. Thermogravimetric analysis (TGA) and differential scanning calorimetry (DSC) were carried out in a controlled atmosphere using the simultaneous differential techniques (SDT) 2960 instrument of TA Instruments. Thermograms were recorded at 4 and 10 K min^{-1} heating rates in air or nitrogen flow. The covered temperature range was from RT to 1273 K.

3. Results and Discussion

3.1. Characterization of α-Al_2O_3 Samples. Powder samples have been characterized by means of XP and DRIFT spectroscopies as well as by means of thermal analysis (TGA-DSC).

The Al(2p) and O(1s) XP peaks lie at 74.2 and 531.0 eV, respectively (see Figure 3), and the BE difference between them is 456.8 eV. All these values are in fair agreement with literature data for Al^{3+} and O^{2-} species in α-Al_2O_3.[25,26] Moreover, the high O/Al surface atomic ratio (1.8) and the asymmetry of the O(1s) band (see the peak tail at high BE in Figure 3) suggest the presence of surface hydroxyl groups.[27,13] In this regard, it has to be emphasized that Suda et al.[28] classified three different types of OH surface groups: (i) free or isolated OH groups, (ii) H-bonded OH groups, and (iii) OH groups interacting with chemisorbed water molecules. The distribution of these groups is a function of preparation conditions such as temperature and sample dehydration degree.

Infrared spectroscopy has been used in the past to investigate the nature of isolated OH groups on low index planes of transition aluminas.[29] The existence of the following species was revealed: (i) OH groups coordinated to a single tetrahedral Al^{3+} site; (ii) OH groups coordinated to a single octahedral Al^{3+} site; (iii) OH groups bridging a tetrahedral

(20) Hoffmann, R. *Solids and Surfaces: A Chemist's View of Bonding in Extended Structures*; VCH: New York, 1988.
(21) Lias, S. G.; Stein, S. E. *NIST/EPA/MSDC Mass Spectral Database*, PC version 3.0; June 1990.
(22) Ko, E. I.; Benzinger, J. B.; Madix, R. J. *J. Catal.* **1980**, *62*, 264.
(23) (a) Kubelka, P.; Munk, F. *Z. Tech. Phys.* **1931**, *12*, 593. (b) Kortum, G. *Reflectance Spectroscopy*; Springer: New York, 1969.
(24) Shirley, D. A. *Phys. Rev.* **1972**, *55*, 4709.
(25) Moulder, J. F.; Stickle, W. F.; Sobol, P. E.; Bomben, K. D. In *Handbook of X-ray Photoelectron Spectroscopy*; Chastain, J., Ed.; Physical Electronics: Eden Prairie, MN, 1992.
(26) *NIST Standard Reference Database 20*, Version 3.0.
(27) McIntyre, N. S.; Chan, T. C. In *Practical Surface Analysis*, 2nd ed.; Briggs, D., Seah, M. P., Eds.; John Wiley and Sons: New York, 1990; Vol. 1, Chapter 10.
(28) Suda, Y.; Morimoto, T.; Nagao, M. *Langmuir* **1987**, *3*, 99.

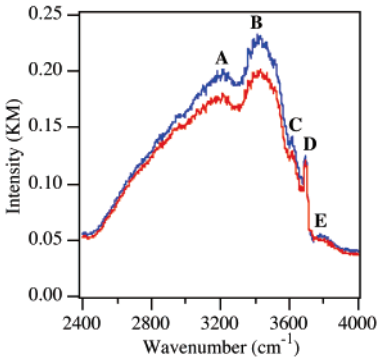

Figure 4. DRIFT spectrum at 4 cm^{-1} resolution of the α-Al_2O_3 powder sample before thermal treatment (blue line) and after heating (red line) in N_2 at 373 K.

and an octahedral site; (iv) OH groups bridging two octahedral sites; (v) capped OH groups, that is, contemporary bridging three octahedral sites.

The O−H stretching region of the DRIFT spectrum of our α-Al_2O_3 powder sample is reported in Figure 4 where bands are alphabetically labeled. The spectrum consists of the following: (i) a very broad and intense band extending from ∼2500 to 3600 cm^{-1} with two evident features around 3220 and 3430 cm^{-1} (A and B, respectively); (ii) two peaks at 3616 and 3695 cm^{-1} (C and D, respectively); (iii) a weak and quite broad band at ∼3770−3800 cm^{-1} (E). Reference to literature data[30] allows us to ascribe the broad and intense band covering the spectral region from 2500 to 3600 cm^{-1} to H-bonded water. Furthermore, the presence of the two features at ∼3220 and 3430 cm^{-1} suggests that water molecules bind to the surface in different ways. Consistently, the DRIFT region including water bending modes (not herein reported) is characterized by the presence of two main contributions at ∼1540 and 1635 cm^{-1}. All the remaining bands of the DRIFT spectrum are assigned to the stretching of isolated and H-bonded OH groups.[29a] More specifically, the narrow peak D is ascribed to OH groups three-fold coordinated to octahedral Al^{3+} sites, while the wider C one is consistent with the presence of H-bonded OH groups. Finally, the weak and rather broad band **E** is associated to the presence of OH groups one-fold coordinated to a single octahedral Al^{3+} site.

Moving to the analysis of TGA data, the inspection of Figure 5 points out that (i) water weakly bonded is lost at temperatures lower than 338−343 K, and (ii) a significant weight loss takes place between 483 and 583 K. In this regard, it should be stressed that the loss of H-bonded OH groups agrees with DRIFT results which show, for α-Al_2O_3 heated at 373 K in a N_2 flow, the decrease of peak C (see Figure 4).

3.2. Reaction of CO_2 with α-Al_2O_3 at Atmospheric Pressure. The spectral region ranging from 1200 to 1800

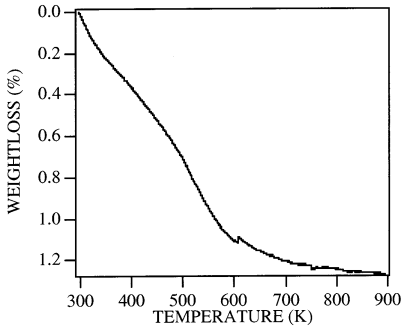

Figure 5. TGA spectrum (air flow, rate = 10 K × min^{-1}) of the α-Al_2O_3 powder sample.

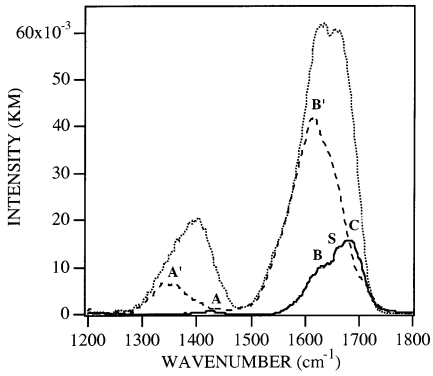

Figure 6. DRIFT spectrum at 4 cm^{-1} resolution obtained after chemisorption of CO_2 at RT on the untreated α-Al_2O_3 powder sample (—); chemisorption of CO_2 at 523 K on the α-Al_2O_3 powder sample heated at 523 K in N_2 (- - -); chemisorption of CO_2 at RT on the α-Al_2O_3 powder sample previously heated at 523 K in N_2 (····).

cm^{-1} of the DRIFT spectra of the α-Al_2O_3 powder sample after CO_2 dosing at different temperatures is reported in Figure 6. In the spectrum recorded at RT of the untreated α-Al_2O_3 are evident at least three bands at 1423 (A) cm^{-1}, 1631 (B) cm^{-1}, and 1680 (C) cm^{-1}. Moreover, the lower frequency side of the third band is characterized by the presence of an evident shoulder (S) at ∼1665 cm^{-1}. The position of these bands is indicative of the formation of surface-bicarbonate species[30−32] as a consequence of the interaction between OH surface groups and CO_2. In the same figure, the DRIFT spectrum of the α-Al_2O_3 powder sample treated for 2 h in N_2 at 523 K and exposed to CO_2 either at 523 K or at RT is also reported. The spectrum of α-Al_2O_3 heated at 523 K and exposed to CO_2 at the same temperature is characterized by only two broad bands (∼1352 cm^{-1} (A′) and 1620 (B′) cm^{-1}), whose position is consistent with the presence of surface BCC.[33] At variance to that, the DRIFT spectrum of the α-Al_2O_3 sample treated for 2 h in N_2 at 523 K but exposed to CO_2 at RT reveals the coexistence of both surface bicarbonate and BCC. Such a behavior suggests that (i) the surface dehydroxylation has a reversible character,

(29) (a) Boehm, H.-P.; Knözinger, H. In *Catalysis: Science and Technology*; Anderson, J. R., Boudart, M., Eds.; Springer-Verlag: New York, 1983; Vol. 4, Chapter 2. (b) Zecchina, A. *Discuss. Faraday Soc.* **1971**, *52*, 89. (c) Borello, E.; Cimino, A.; Ghiotti, G.; LoJacono, M.; Schiavello, M.; Zecchina, A. *Discuss. Faraday Soc.* **1971**, *52*, 149. (d) Morterra, C.; Ghiotti, G.; Garrone, G.; Boccuzzi, F. *J. Chem. Soc., Faraday Trans. 1* **1976**, *72*, 2722.
(30) Little, L. H. In *Infrared Spectra of Adsorbed Species*; Academic Press: San Diego, CA, 1966; Chapter 3.
(31) (a) Gatehouse, B. M.; Livingstone, S. E.; Nyholm, R. S. *J. Chem. Soc.* **1958**, 3137. (b) Morterra, C.; Zecchina, A.; Coluccia, S.; Chiorino, A. *J. Chem. Soc., Faraday Trans. 1* **1977**, *73*, 1544. (c) Morterra, C.; Cerrato, G.; Bolis, V.; Fubini, B. *Spectrochim. Acta* **1993**, *49A*, 1269.
(32) The DRIFT spectral region ranging from 3000 to 3550 cm^{-1} (not reported) includes weak contributions attributable to the O−H stretching of surface bicarbonates.
(33) Seiferth, O.; Wolter, K.; Dillmann, B.; Klivenyi, G.; Freund, H.-J.; Scarano, D.; Zecchina, A. *Surf. Sci.* **1999**, *421*, 176.

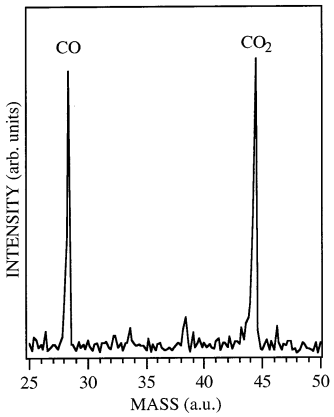

Figure 7. QM spectrum of volatile products after chemisorption of CO_2 at RT on partially reduced α-Al_2O_3.

and (ii) the surface reactivity of alumina can be strongly influenced by its thermal history and preparation procedure. Moreover, experimental evidence pertaining to the chemisorption of CO_2 at RT on the untreated sample is indicative of a situation entirely different with respect to the one we theoretically modeled (see later). At variance to that, DRIFT data concerning the chemisorption of CO_2 at 523 K on a powder formerly dehydroxylated are quite well suited to be rationalized by means of our theoretical calculations.

3.3. Reaction of α-Al_2O_3 with CO_2 in HV Conditions. The Al(2p) XP spectrum obtained after the activation treatment is shown in Figure 3. In addition to the signal attributed to the Al^{3+} in α-Al_2O_3, a lower BE contribution at 73.4 eV is also evident. This feature suggests that the heating treatment, besides removing surface OH groups (see the decrease of the O(1s) peak tail), has also the effect of partially reducing the sample through the creation of surface O vacancies. Accordingly, the O/Al surface atomic ratio passes from 1.8 (see previous description) to 1.0.

As already pointed out, the activated surface was exposed to CO_2 at a pressure of 10^{-4} Pa, and the reaction products were characterized by means of QMS. The QM spectrum reported in Figure 7 clearly shows the presence of both CO_2 ($m/e = 44$ amu) and CO ($m/e = 28$ amu).[34]

After the CO_2 dosing, the Al(2p) and O(1s) XPS bands become narrower, the value of the surface O/Al atomic ratio increases from 1.0 to 1.7, and the maxima of the Al(2p) and O(1s) peaks move in opposite directions. All of this evidence suggests a less defective surface and a reconditioning of the surface stoichiometry after the CO_2 exposure. Finally, it is interesting to observe that the shape of the O(1s) peak does not change after the chemisorption; in particular, no feature attributable to OH groups is present.

3.4. Theoretical Results. Our first concern was that of checking the capability of **I** of mimicking the clean surface, and, in particular, of reproducing the well-known strong relaxation undergone by the topmost layer of α-Al_2O_3-(0001).[8a−d] For this purpose, we optimized the coordinates

(34) It is interesting to note that the chemisorption of CO on a stoichiometric, well-ordered $(V_{0.985}Cr_{0.015})_2O_3(0001)$ surface gives rise to irreversible changes in the surface. In particular, the adsorbate abstracts lattice oxygen, it reduces the surface, and it desorbs as CO_2.[35]

Table 1. Atomic Displacements (Å) from the Bulk Compared with Experiments and Various Cluster and Slab Calculations

			CLUSTER			SLAB
atom	this work	expt	HF[c]	B3LYP[c]	GGA[d]	LDA[e]
$L^a_{s1}(z)$	−0.54	−0.34[a]	−0.58	−0.54	−0.53	−0.71
$L^a_{s2}(z)$	−0.54					
$L^b_{s1}(x)$	0.02	0.07[a]			0.05	−0.03
$L^b_{s1}(y)$	0.06	0.20[a]			0.00	−0.07
$L^b_{s1}(z)$	0.02	0.09[a]	0.00	0.04	0.03	−0.01
L^b_{s2}	0.05					
L^b_{s2}	0.06					
L^b_{s2}	0.03					
d_1[f]	0.28	0.42[a]/0.3[b]	0.25	0.25	0.27	0.12
d_2[f]	0.27					
$r(L^a_{s1}-L^b_{s1})$	1.70	1.77[a]/1.72[b]	1.73	1.75	1.72	1.66
$r(L^a_{s2}-L^b_{s2})$	1.72					
$\Delta r(L^a_{s1}-L^b_{s1})$	−0.15	−0.08[a]/−0.13[b]	−0.12	−0.10	−0.13	−0.17
$\Delta r L^a_{s1}-L^b_{s1})$	−0.13					

[a] Reference 8b. [b] Reference 8a. [c] Reference 8g. [d] Reference 8p. [e] Reference 8j. [f] The *d* parameter defines the spacing between the first and second layers.

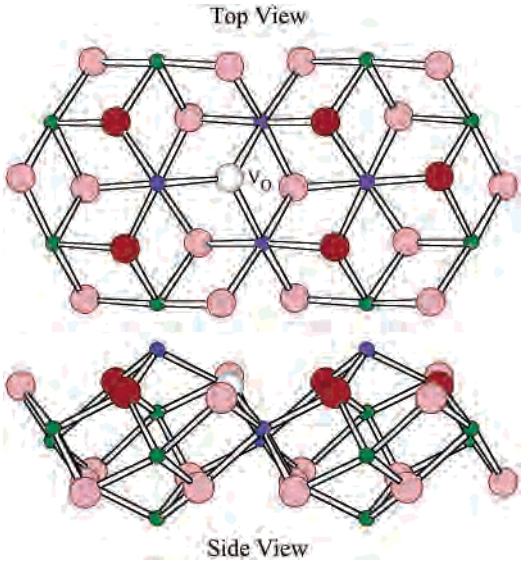

Figure 8. Schematic representation of the unrelaxed cluster $Al_{14}O_{21}$ ($\mathbf{I}^F$). Al (O) atoms in green (pink) are saturated. Pseudo-atom saturators are not displayed for the sake of clarity.

of the two L^a_s's as well as of the six nonsaturated L^b_s's (the O atoms in red in Figure 2) of **I**. Computed quantities compare well with literature experimental and theoretical values[8g,j,p] (see Table 1); moreover, the main features of the electronic structure of **I** are very similar to those pertaining to the Al_8O_{12} cluster we adopted in ref 8p. The interested reader may refer to this reference for a detailed discussion.

As already mentioned, polycrystalline α-Al_2O_3 is usually characterized by the presence of F centers which should be present in a significant amount on the surface of the activated sample (see preceding discussion). Thus, to understand, at least at a semiquantitative level, how the electronic structure of the stoichiometric clean surface is perturbed upon the creation of a neutral F center, we performed a further series of calculations on the saturated $Al_{14}O_{21}$ cluster ($\mathbf{I}^F$, see Figure 8) obtained from **I** by removing L^b_{s11}. In these numerical experiments, the coordinates of L^a_s (two atoms) and L^b_s (five atoms) were optimized without imposing any constraint.

Table 2. Hirshfeld Charges of Selected Atoms in **I** and $\mathbf{I}^F$

	I	$\mathbf{I}^F$
L^a_{s1}	0.66	0.44
L^a_{s2}	0.66	0.66
Al_{CC1}	0.43	0.38
Al_{CC2}	0.45	0.43
L^b_{s2}	−0.36	−0.36
L^b_{s1}	−0.36	−0.38

The comparison of geometrical parameters of **I** and $\mathbf{I}^F$ indicates only minor variations on passing from the defect-free surface to the one representative of a surface F center, with one exception: a significant shift (0.27 Å) of L^a_{s1} in the direction of V_O. Incidentally, this is perfectly in tune with data reported by Stashans et al.[10c] and Xu et al.[10b] for F centers in bulk α-Al_2O_3.

Hirshfeld[36] charges (Q_H) of selected atoms of **I** and $\mathbf{I}^F$ (see Table 2) point out that only the V_O nearest neighbors (L^a_{s1}, Al_{CC1}, and Al_{CC2}) are perturbed by the creation of the F center. According to that, the DOS/PDOS of **I** and $\mathbf{I}^F$ (see Figure 9, top and middle) are rather similar, even if the band gap of $\mathbf{I}^F$ is characterized by the presence of an occupied state, completely localized on the V_O nearest neighbors (see Figure 9 bottom) and 1.6 eV above the valence band maximum. Incidentally, this ΔE is rather similar to experimental (3.0 eV)[10d] and theoretical (3.45 eV)[10b] data pertaining to neutral F centers in bulk α-Al_2O_3.

A deep understanding of the bonding interaction between CO_2 and the defect-free α-Al_2O_3(0001) surface requires a detailed knowledge of the electronic structure of the free adsorbate. For this reason, let us briefly summarize the results obtained by running DFT calculations on the isolated CO_2 with $D_{\infty h}$ symmetry. The valence manifold of CO_2 (see Figure 10) includes a total of eight MOs ($2\sigma_g$, $2\sigma_u$, $1\pi_u$, $1\pi_g$, $2\pi_u$). Among them, the $1\pi_g$ HOMO is C−O nonbonding in character, while the $2\pi_u$ LUMO is strongly C−O antibonding (see COOPs in Figures 10 and 2D contour plots in Figure 11). As far as the agreement between experiment and theory is concerned, both structural and vibrational parameters are satisfactorily reproduced: BL(C−O_{exp}/C−O_{theo}) = 1.163/1.174 Å;[37] $\nu_{1(exp)}/\nu_{1(theor)}$ = 1337/1307 cm^{-1}, $\nu_{2a(exp)}/\nu_{2a(theor)}$ = 667/637 cm^{-1}, $\nu_{2b(exp)}/\nu_{2b(theor)}$ = 667/638 cm^{-1}; $\nu_{3(exp)}\nu_{3(theor)}$ = 2349/2338 cm^{-1}.[38] Finally, C and O Mulliken[39] (Hirschfeld)[36] charges are 0.95/−0.47 (0.30/−0.15).

On the basis of simple symmetry and overlap considerations, we can foresee that CO_2 frontier orbitals (the $1\pi_g$ and $2\pi_u$ MOs) will be certainly the most perturbed upon chemisorption; nevertheless, their entanglement in the adsorbate−substrate interaction should differently affect the C−O bond. More specifically, the involvement of the HOMO in the $CO_2 \rightarrow L^a_s$ donation should perturb to a negligible extent the C−O bond length (BL), while the opposite should be true as far as the participation of the $2\pi_u$ CO_2 LUMO to the $L^b_s \rightarrow CO_2$ back-donation is concerned.

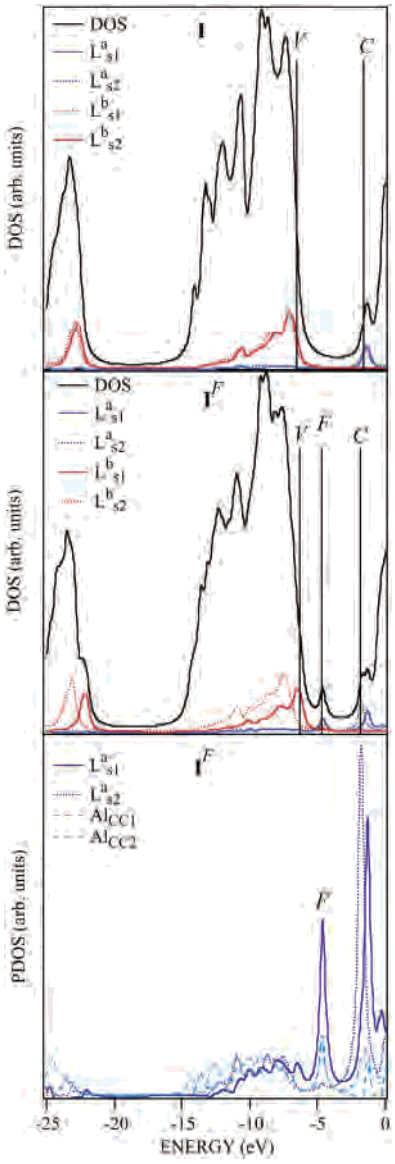

Figure 9. DOS of the saturated clusters **I** and $\mathbf{I}^F$. PDOSs of L^a_s, L^b_s, and Al_{CC} are also included. V, F, and C account for the valence band top, the F state due to the O vacancy, and the conduction band bottom, respectively.

Before moving to the analysis of data pertaining to the α-Al_2O_3(0001)−CO_2 interaction, let us emphasize that neither theoretical nor experimental information concerning the arrangement of CO_2 on α-Al_2O_3 single crystal surfaces is available. Such a lack forced us to perform a series of numerical experiments with different starting geometries (see Figure 12).[40] Among them, the only arrangement giving rise to a stable CO_2−surface complex was the BCC_1 sketched in Figure 13. Optimized geometrical parameters (see Figure 13 and Table 3) indicate that both the adsorbate and the substrate are strongly perturbed upon chemisorption. In particular: (i) the CO_2 is strongly bent; (ii) the C−O1, C−O2, and L^a_{s1}−L^b_{s11} BLs are significantly lengthened; (iii)

(35) Toledano, D. S.; Henrich, V. E.; Metcalf, P. *J. Vac. Sci. Technol., A* **2000**, *18*, 1906.
(36) (a) Hirshfeld, F. L. *Theor. Chim. Acta* **1977**, *44*, 1703. (b) Wiberg, K. B.; Rablen, P. R. *J. Comput. Chem.* **1993**, *14*, 1504.
(37) Wells, A. F. *Structural Inorganic Chemistry*, 5th ed.; Clarendon Press: Oxford, 1984.
(38) Taylor, J. H.; Benedict, W. S.; Strong, J. *J. Chem. Phys.* **1952**, *20*, 1884.
(39) Mulliken, R. S. *J. Chem. Phys.* **1955**, *23*, 1833.

(40) In Figure 12, we have only reported, among the starting geometries we considered, those corresponding to BCC surface complexes.

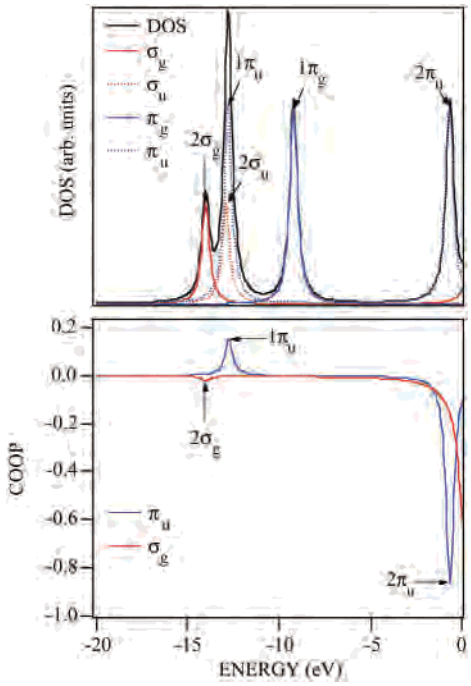

Figure 10. DOS (top) and C−O COOP (bottom) of the free CO_2. σ and π contributions to the DOS and COOP are also outlined. Vertical bars represent the energy of the highest occupied MO (HOMO). MOs $1\sigma_g$ and $1\sigma_u$ lie out of the reported energy range.

Table 3. Variation in Height (Δz) and in BL (Δr) of L_s^a and L_s^b upon Chemisorption of CO_2 on Al_2O_3(0001)

	Δz (Å)	Δr (Å)
L_{s1}^a	0.40	
L_{s2}^a	0.20	
L_{s11}^b	0.19	
$L_{s1}^a-L_{s11}^b$		0.20
$L_{s1}^a-L_{s12}^b$		0.01
$L_{s1}^a-L_{s13}^b$		0.01

the inward relaxation of both L_s^a's is partially relieved, even if to a different extent (L_{s1}^a more than L_{s2}^a). As far as the ΔH_{ads} is concerned, the computed value of −15.30 kcal/mol[41] agrees quantitatively with the heat of adsorption obtained by Mao and Vannice for CO_2 on high surface area α-alumina (−16.0 kcal/mol).[42]

Hirshfeld[36] charges of selected atoms of **I**−CO_2 are compared with those of constituent fragments in Table 4. The atomic species undergoing the largest ΔQ_H is L_{s11}^b (0.20), while variations associated with L_{s1}^a, L_{s2}^a, and O2 are definitely smaller (−0.05/−0.07), and no modification is computed for C and O1 atoms. A rationale of this finding has been obtained by performing a further series of calculations on the free CO_2 and by varying the O−C−O bond angle (BA) from 180° to 131°.[43] Despite the absence of a symmetry

(41) Contributions to ΔH_{ads} in eq 2.1 are the following: $\Delta E_{elstat} = -255.45$, $\Delta E_{Pauli} = 461.20$, $\Delta E_{int} = -300.91$, and $\Delta E_{prep} = 76.64$ kcal/mol ($\Delta E_{prep}^{CO_2}$ and ΔE_{prep}^{I} are 49.23 and 27.41 kcal/mol, respectively), while BSSE amounts to 3.22 kcal/mol.

(42) Mao, C.-F.; Vannice, M. A. *Appl. Catal., A* **1994**, *111*, 151.

(43) The results of these calculations pointed out that low lying CO_2 $1\pi_u$ and $1\pi_g$ MOs are only slightly perturbed upon the bending, whereas the in-plane component (a′) of the $2\pi_u$ LUMO is strongly stabilized (it acquires a partial O−O bonding character) with respect to the a″ partner which is perpendicular to the CO_2 plane.

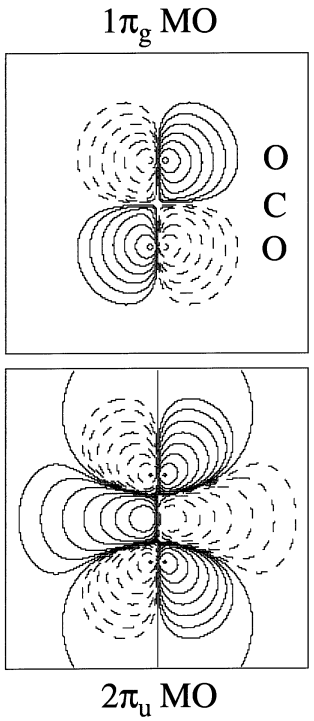

Figure 11. 2D contour plots of one component of the CO_2 $1\pi_g$ HOMO (top) and $2\pi_u$ LUMO (bottom). Contour values are ±0.48, ±0.24, ±0.12, ±0.06 ... $e^{1/2} \times Å^{-3/2}$ with negative values in dashed lines.

Table 4. Comparison of Hirshfeld Charges of Selected Atoms in **I** and **I**−CO_2

atom	**I**	**I**−CO_2	Δ
L_{s1}^a	0.66	0.59	−0.07
L_{s2}^a	0.66	0.60	−0.06
L_{s11}^b	−0.36	−0.14	0.20
L_{s12}^b	−0.36	−0.37	−0.01
L_{s13}^b	−0.36	−0.37	−0.01
	Free Molecule		
C	0.30	0.30	0.00
O_1	−0.15	−0.15	0.00
O_2	−0.15	−0.20	−0.05

plane in the **I**−CO_2 cluster, this new series of calculations allowed us to discriminate the participation of the in-plane (a′) and out-of-plane (a″) partners of CO_2 frontier orbitals in the adsorbate−substrate interaction. In this regard, the PDOS and COOP reported in Figure 14 reveal that (i) the a′ component of the CO_2 $2\pi_u$ LUMO is dramatically stabilized upon chemisorption as a consequence of the $L_{s11}^b \rightarrow CO_2$ back-donation,[44] and (ii) the adsorbate → substrate donation, a multicenterd interaction involving both adsorbate O atoms and both L_s^a's (the O−L_{s2}^a BL is 2.17 Å), is weaker than the substrate → adsorbate back-donation. As a whole, the $L_{s11}^b \rightarrow CO_2$ transfer of charge is partially offset by the $L_{s1}^a \leftarrow CO_2 \rightarrow L_{s2}^a$ interaction, thus explaining ΔQ_H values of Table 4.

Asymmetrical (1690 cm^{-1}) and symmetrical (1202 cm^{-1}) C−O stretching frequencies computed for the BCC_1 adduct are in semiquantitative agreement with DRIFT measurements

(44) The ΔE between the a′ component of the $2\pi_u$ and $1\pi_g$ MOs in the free CO_2 with an O−C−O BA of 131° amounts to ∼3.5 eV, while it is negligible in the chemisorbed species.

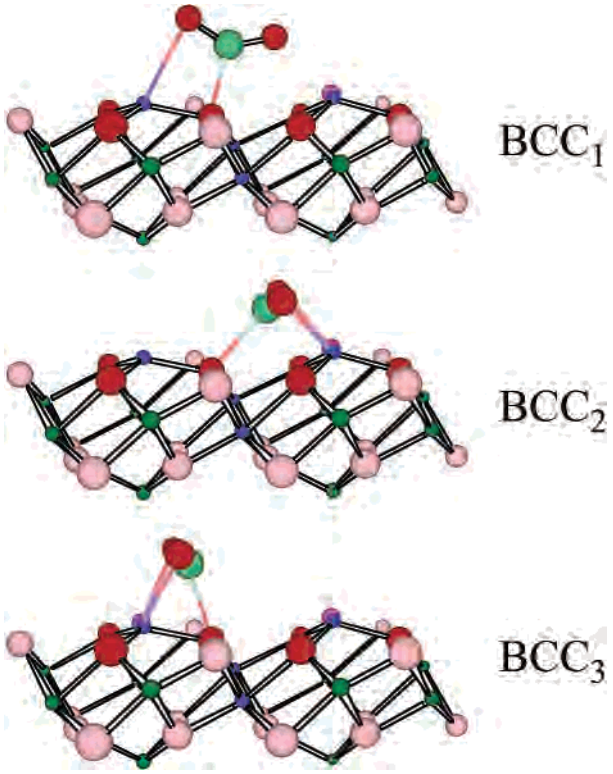

Figure 12. Schematic representation of possible BCC species possibly produced by the interaction of CO_2 with dehydroxylated α-Al_2O_3.

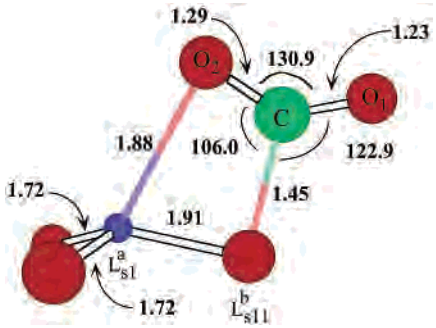

Figure 13. Structural parameters (bond lengths in Å and bond angles in deg) of the optimized BCC_1 surface complex.

pertaining to dehydroxylated α-Al_2O_3 exposed to CO_2 at 523 K (bands **B′** and **A′** of Figure 6) as well as with FTIR data reported by Morterra et al. for dehydroxylated α-Al_2O_3 (1710−1310 cm^{-1}).[11b] We also computed the BCC_1 bending mode (847 cm^{-1}) which cannot be compared with experimental data because vibrations of the substrate lattice are present in the same energy range. In any case, the significant blue shift of this mode compared to the ν_2 value of the free CO_2[38] is consistent with the proposed adsorbate−substrate bonding scheme.

We turn now our attention to the chemisorption of CO_2 on partially reduced α-Al_2O_3. This has been modeled by assuming the formation of a surface carbonate where one of the adsorbate O atoms saturates the coordinative vacancies induced by the V_O creation (see Figure 15a). The coordinates of the adsorbate, L_s^a, and L_s^b have been then optimized without any constraint. Interestingly, the final geometry (see Figure 15b) corresponds to the reduction of CO_2 to CO and to the restoration of the stoichiometric surface. Moreover,

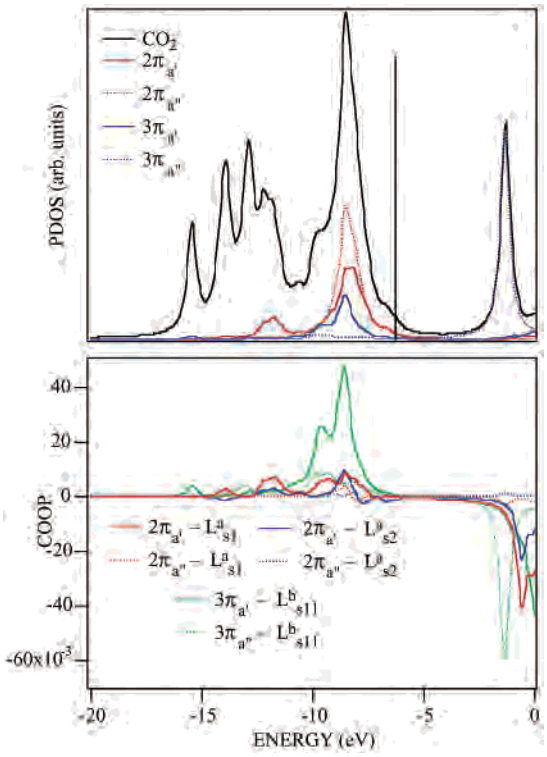

Figure 14. DOS (top) and COOP (bottom) of the chemisorbed CO_2. Levels reminiscent of the free CO_2 HOMO ($2\pi_{a'}$ and $2\pi_{a''}$ levels) and LUMO ($3\pi_{a'}$ and $3\pi_{a''}$ levels) are outlined. Vertical bars represent the energy of the HOMO of the **I**−CO_2 cluster.

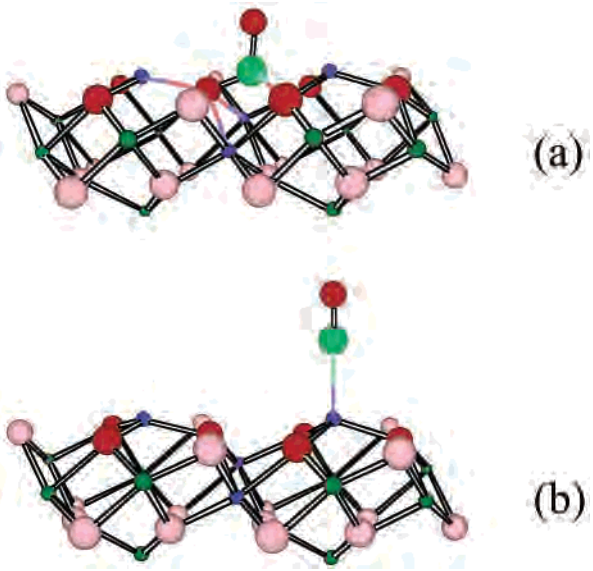

Figure 15. Schematic representation of the starting (a) and optimized (b) geometry of the $\mathbf{I}^F$−CO_2 cluster.

the final CO surface complex is characterized by geometrical parameters equivalent to those reported in ref 8p, and reaction 3.1 is computed to be exothermic by ∼59 kcal/mol.

$$\alpha\text{-}Al_2O_{3-x}(0001) + CO_2 \rightarrow \alpha\text{-}Al_2O_3(0001) + CO \qquad (3.1)$$

4. Conclusions

The chemisorption of CO_2 on polycrystalline, dehydroxylated α-Al_2O_3 has been experimentally and theoretically investigated by combining XPS, DRIFT, and QMS results

with the outcomes of DFT calculations carried out for CO_2 interacting with the α-Al_2O_3(0001) surface. The CO_2− substrate interaction gives rise to a surface bidentate-chelating carbonate whose bonding scheme is dominated by a surface → adsorbate back-donation assisted by a definitely weaker adsorbate → surface donation. Both the electronic and structural properties of the substrate are significantly perturbed upon chemisorption, thus providing a theoretical rationale of the CO_2 inadequacy to probe the basicity of surface Lewis base sites. As far as the interaction of CO_2 with partially reduced α-Al_2O_3 is concerned, both experimental and theoretical results are consistent with a reduction of the adsorbate to CO and the concomitant restoration of the surface stoichiometry. As a whole, the obtained results exemplify the power of combined theoretical and experimental investigations where neither technique leads, but rather, they are used in parallel to gain further insight than either could on its own.

IC0257773